Frequency Divider

Federico Milano, *Fellow, IEEE*, Álvaro Ortega, *Student Member, IEEE*

***Abstract*— The paper proposes an approximated yet reliable formula to estimate the frequency at the buses of a transmission system. Such a formula is based on the solution of a steady-state boundary value problem where boundary conditions are given by synchronous machine rotor speeds and is intended for applications in transient stability analysis. The hypotheses and assumptions to define bus frequencies are duly discussed. The rationale behind the proposed frequency divider is first illustrated through a simple 3-bus system. Then the general formulation is duly presented and tested on two real-world networks, namely a 1,479-bus model of the all-island Irish system and a 21,177-bus model of the European transmission system.**

***Index Terms*— Frequency estimation, quasi-static phasor model, dq-frame model, transient stability analysis, center of inertia.**

I. Introduction

A. Motivations

The conventional power system model for transient stability analysis is based on the assumption of quasi-steady-state phasors for voltages and currents. The crucial hypothesis on which such a model is defined is that the frequency required to define all phasors and system parameters is constant and equal to its nominal value. This model is appropriate as long as only the rotor speed variations of synchronous machines is needed to regulate the system frequency through standard primary and secondary frequency regulators. In recent years, however, an increasing number of devices other than synchronous machines are expected to provide frequency regulation. These include, among others, distributed energy resources such as wind and solar generation [1]–[5]; flexible loads providing load demand response [6], [7]; HVDC transmission systems [8]–[10]; and energy storage devices [11]–[13]. However, these devices do not generally impose the frequency at their connection point with the grid. There is thus, from a modeling point of view, the need to define with accuracy the local frequency at every bus of the network. This paper provides an accurate yet simple and computationally inexpensive formula to estimate such frequencies and, thus, improve the fidelity of the conventional power system model for transient stability analysis.

B. Literature Review

The most common way to estimate the system frequency in transient stability analysis is the evaluation of the center of inertia (COI) which is an arithmetic mean of rotor speeds of synchronous machines weighted through their inertia constants. The frequency of the COI is well-accepted and widely used in the literature on transient and frequency stability analysis. We cite, for example, [14] and [15]. While the COI is particularly useful to define the frequency of clusters of coherent machines, it cannot capture local oscillations and is thus not adequate to implement and simulate the frequency controllers discussed in the motivations above.

Another common approach consists in defining the numerical derivative of the phase angle of bus voltage phasors through some sort of filtering, e.g., a washout filter. This approach was first discussed in [16] along with the COI model, and is commonly used in proprietary software tools for power system simulation, e.g., [17].

The issues of the numerical differentiation of voltage angles are well known. The literature on this subject has mainly focused on the definition of analytical expressions, e.g., [18], or more accurate numerical methods, e.g., [19], to define the derivative of the bus voltage angles. The common starting point of the two references above, as well as of this paper, is the expression that links bus voltage phasors and current injections at buses through the network admittance matrix. We propose an analytical expression which is not model-dependent as that given in [18] and is considerably simpler, but consistent with standard approximations used in power system models for transient stability analysis.

C. Contributions

The novel contributions of the paper are twofold.

- An approximated yet reliable and simple formula to estimate the frequency at all buses of the system. The proposed formula is aimed to improve transient stability analysis models.
- A detailed comparison of the accuracy and the computational burden of the proposed frequency divider formula, the commonly-used washout filters utilized to estimate the numerical derivative of bus voltage phase angles as well as the COI frequency. Such a comparison is based on both quasi-static phasor and dq-frame power system models.

D. Paper Organization

The remainder of the paper is organized as follows. Section II duly discusses the rationale, the hypotheses and assumptions required to obtain the proposed frequency divider formula. Section III illustrates, through a simple example, the validity of the frequency divider and tests it considering different scenarios and load models. Section IV presents simulation results based on two real-world systems, namely a 1,479-bus model of the all-island Irish system and a 21,177-bus model of the European ENTSO-E transmission system. Conclusions are drawn in Section V.

Federico Milano and Álvaro Ortega are with the School of Electrical and Electronic Engineering, University College Dublin, Ireland. E-mails: (federico.milano@ucd.ie; alvaro.ortega-manjavacas@ucdconnect.ie)

II. Frequency Divider Formula

In this section, we develop a simple, yet effective general analytical expression to estimate the frequency deviations at every location of the network. Subection II-A discusses the theoretical background and the rationale behind the proposed formula. The analytical derivation is then discussed in details in Subsection II-B

A. Rationale

During a transient triggered by a large disturbance, e.g., the occurrence of a fault followed by its clearance, synchronous machine rotor speeds oscillate. It is well known that, during a transient, each machine shows interarea oscillation modes common to its coherent group as well as local non-dominant modes [14]. The key point is that, during the transient, machine frequencies are not equal and, hence, the frequency cannot be the same everywhere in the system. However, due to the common approximations of the conventional transient stability model, only the frequencies – effectively, the rotor speeds – of the internal electromotive forces (emfs) of synchronous machines can be determined by means of the time integration of the power system model.

In [20] and, later, in [21], the author posed the basis for the modeling of the transmission system as a *continuum* where the speeds of synchronous machines are the *boundary conditions* that the frequency has to satisfy. We base the definition of the frequency divider formula on such a continuum. However, since we are interested in electromecanical transients and in the time scale associated to such dynamics, we assume that the wave propagation is faster than the electromechanical modes of synchronous machines and, thus, we neglect transient effects of wave propagation, e.g., reflection.[1] As a consequence, we assume that, to compute the spatial variations of the frequency, the problem that can be solved is **a steady-state boundary value problem, where boundary conditions are given by synchronous machine rotor speeds.** This assumption is consistent with quasi-steady-state phasors and lumped transmission line models assumed to solve power system transient stability analysis.

B. Analytical Derivation

The very starting point is the augmented admittance matrix, with inclusion of synchronous machine internal impedances as it is commonly defined for fault analysis [22]. System currents and voltages are linked as follows:

$$\begin{bmatrix} \bar{\boldsymbol{i}}_G \\ \bar{\boldsymbol{i}}_B \end{bmatrix} = \begin{bmatrix} \bar{\mathbf{Y}}_{GG} & \bar{\mathbf{Y}}_{GB} \\ \bar{\mathbf{Y}}_{BG} & \bar{\mathbf{Y}}_{BB} + \bar{\mathbf{Y}}_{B0} \end{bmatrix} \begin{bmatrix} \bar{\boldsymbol{e}}_G \\ \bar{\boldsymbol{v}}_B \end{bmatrix} \tag{1}$$

where $\bar{\boldsymbol{v}}_B$ and $\bar{\boldsymbol{i}}_B$ are bus voltages and current injections, respectively, at network buses; $\bar{\boldsymbol{i}}_G$ are generator current injections; $\boldsymbol{e}_G$ are generator emfs behind the internal generator impedance; $\bar{\mathbf{Y}}_{BB}$ is the standard network admittance matrix; $\bar{\mathbf{Y}}_{GG}$, $\bar{\mathbf{Y}}_{GB}$ and $\bar{\mathbf{Y}}_{BG}$ are admittance matrices obtained using the internal impedances of the synchronous machines; and $\bar{\mathbf{Y}}_{B0}$ is a diagonal matrix that accounts for the internal impedances of the synchronous machines at generator buses.[2] All quantities in (1) depend on the frequency. However, the dependency of the admittance matrices above on the frequency is neglected. This approximation has a very small impact on the accuracy of the frequency estimation and allows determining a compact expression of bus frequencies, as discussed in the remainder of this section.

To further elaborate on (1), let us assume that load current injections $\bar{\boldsymbol{i}}_B$ can be neglected in (1). This is justified by the fact that the equivalent load admittance, in trasmission systems, is typically one order of magnitude smaller than that of the diagonal elements of $\bar{\mathbf{Y}}_{BB} + \bar{\mathbf{Y}}_{B0}$. This appears as a critical assumption, and for this reason we test its adequateness in the examples of Section III, where we consider a variety of load models, including nonlinear dynamic ones. Hence, we rewrite (1) as follows:

$$\begin{bmatrix} \bar{\boldsymbol{i}}_G \\ \mathbf{0} \end{bmatrix} = \begin{bmatrix} \bar{\mathbf{Y}}_{GG} & \bar{\mathbf{Y}}_{GB} \\ \bar{\mathbf{Y}}_{BG} & \bar{\mathbf{Y}}_{BB} + \bar{\mathbf{Y}}_{B0} \end{bmatrix} \begin{bmatrix} \bar{\boldsymbol{e}}_G \\ \bar{\boldsymbol{v}}_B \end{bmatrix} \tag{2}$$

Bus voltages $\bar{\boldsymbol{v}}_B$ are thus a function of generator emfs and can be computed explicitly:

$$\begin{aligned} \bar{\boldsymbol{v}}_B &= -[\bar{\mathbf{Y}}_{BB} + \bar{\mathbf{Y}}_{B0}]^{-1} \bar{\mathbf{Y}}_{BG} \bar{\boldsymbol{e}}_G \\ &= \bar{\mathbf{D}}\, \bar{\boldsymbol{e}}_G \end{aligned} \tag{3}$$

In [18], the relation between generator voltages and currents is exploited to determine the time derivative of load voltages. We proceed in a different way.

Let us consider the time derivative – indicated with the functional $\mathrm{p}(\cdot)$ – of the bus voltage phasors in a dq-frame rotating with frequency ω_0 [24]:

$$\mathrm{p}\bar{v}_{\mathrm{dq},h} = \frac{d}{dt}\bar{v}_{\mathrm{dq},h} + j\omega_0 \bar{v}_{\mathrm{dq},h} \tag{4}$$

where $\bar{v}_{\mathrm{dq},h} = v_{\mathrm{d},h} + j v_{\mathrm{q},h}$. A similar expression can be also obtained using a first order dynamic phasor approximation (see, for example, [25] and [26]).

The first element on the right-hand side of (4) is the time derivative of $\bar{v}_{\mathrm{dq},h}$, which is rotating with the dq-frame, while the second element is the derivative of the dq-frame itself. We now assume the following:

- The quasi-steady-state phasor can be approximated, during an electromechanical transient, to the dq-frame quantity, hence:

$$\bar{v}_h \approx \bar{v}_{\mathrm{dq},h} \tag{5}$$

  Note that in stationary conditions the equality $\bar{v}_h = \bar{v}_{\mathrm{dq},h}$ holds.

[1] In [20], the speed of traveling waves is estimated to be roughly $1,000$ m/s. Thus wave propagation transients can actually overlap fast interarea oscillation modes on long transmission lines. However, accounting for the effect of wave propagation is beyond the scope of this paper.

[2] The non-zero elements of matrices $\bar{\mathbf{Y}}_{GG}$, $\bar{\mathbf{Y}}_{GB}$, $\bar{\mathbf{Y}}_{BG}$ and $\bar{\mathbf{Y}}_{B0}$ are defined through the internal reactances of the synchronous machines in the same way as in the standard fault analysis (see, for example, [22] and [23]). If the machine is not symmetrical, an average of the d- and q-axis internal reactances are used. For example, for a 6^{th} order model, one has $x_G = 0.5(x''_d + x''_q)$.

- The voltage is a sinusoid with time-varying pulsation and its time derivative in (4) is approximated with:

$$\frac{d}{dt}\bar{v}_{\mathrm{dq},h} \approx j\Delta\omega_h \bar{v}_{\mathrm{dq},h} \tag{6}$$

where $\Delta\omega_h$ is the frequency deviation with respect to the reference frequency ω_0 at bus h.

Equation (6) descends from the hypothesis of assuming "slow" variations of the frequency in the system and is consistent with the standard electromechanical power system model utilized for transient stability analysis.

Merging together (4), (5) and (6) leads to:

$$\mathrm{p}\,\bar{v}_h \approx j\,\omega_h\,\bar{v}_h \tag{7}$$

where $\omega_h = \omega_0 + \Delta\omega_h$ is the frequency at bus h. Expressions similar to (7) hold for all other ac quantities in the systems, i.e., generator emfs $\bar{e}$ and currents. For example:

$$\mathrm{p}\,\bar{e}_i \approx j\,\omega_i\,\bar{e}_i \tag{8}$$

where ω_i is the rotor speed of generator i.

We now use the approximated time derivatives (7) and (8) along with network constraints (3) to determine the frequency divider. In particular, differentiating (3) with respect to time leads to:

$$\mathrm{p}\bar{\boldsymbol{v}}_B = \mathrm{p}[\bar{\mathbf{D}}\cdot\bar{\boldsymbol{e}}_G] = \mathrm{p}\bar{\mathbf{D}}\cdot\bar{\boldsymbol{e}}_G + \bar{\mathbf{D}}\cdot\mathrm{p}\bar{\boldsymbol{e}}_G \tag{9}$$

$$\Rightarrow\quad \mathrm{p}\bar{\boldsymbol{v}}_B \approx \bar{\mathbf{D}}\cdot\mathrm{p}\bar{\boldsymbol{e}}_G \tag{10}$$

$$\Rightarrow\quad \frac{d}{dt}\bar{\boldsymbol{v}}_B + j\omega_0\bar{\boldsymbol{v}}_B \approx \bar{\mathbf{D}}\cdot\frac{d}{dt}\bar{\boldsymbol{e}}_G + j\omega_0\bar{\mathbf{D}}\cdot\bar{\boldsymbol{e}}_G \tag{11}$$

$$\Rightarrow\quad j\,\mathrm{diag}(\Delta\boldsymbol{\omega}_B)\,\bar{\boldsymbol{v}}_B \approx j\,\bar{\mathbf{D}}\cdot\mathrm{diag}(\Delta\boldsymbol{\omega}_G)\,\bar{\boldsymbol{e}}_G \tag{12}$$

where:

- in (9), it is assumed that $\mathrm{p}\bar{\mathbf{D}} \approx \mathbf{0}$, i.e., constant transmission line, transformer, load and generator parameters;
- in (10), the time derivative $\mathrm{p}(\cdot)$ is expanded using (4);
- in (11), (3) is utilized to eliminate the terms $j\omega_0\bar{\boldsymbol{v}}_B$ and $j\omega_0\bar{\mathbf{D}}\cdot\bar{\boldsymbol{e}}_G$; and
- $\mathrm{diag}(\cdot)$ indicates a matrix where diagonal elements are the elements of its argument vector.

Finally, based on (6), (7) and (8), $\Delta\boldsymbol{\omega}_B$ and $\Delta\boldsymbol{\omega}_G$ are:

$$\begin{aligned}\Delta\boldsymbol{\omega}_B &= \boldsymbol{\omega}_B - \omega_0\cdot\mathbf{1}\\ \Delta\boldsymbol{\omega}_G &= \boldsymbol{\omega}_G - \omega_0\cdot\mathbf{1}\end{aligned} \tag{13}$$

The set of equations (12) and (13) allows determining the bus voltage frequencies $\boldsymbol{\omega}_B$. In fact, $\bar{\mathbf{D}}$ are parameters and $\boldsymbol{\omega}_G$, $\bar{\boldsymbol{v}}_B$ and $\bar{\boldsymbol{e}}_G$ are variables determined by integrating the set of DAEs describing the power system. While solvable, (12) can be significantly simplified without a relevant loss of accuracy. The following approximations and assumptions are applied:

- $\bar{\boldsymbol{v}}_B \approx \mathbf{1}$ pu and $\bar{\boldsymbol{e}}_G \approx \mathbf{1}$ pu;[3]
- The conductances of the elements of all admittance matrices utilized to compute $\bar{\mathbf{D}}$ are negligible, e.g., $\bar{\mathbf{Y}}_{BB} \approx j\mathbf{B}_{BB}$;

[3]Note that this assumption is acceptable for detailed machine models, e.g., 4th and 6th order. For the classical electromechanical model of the synchronous machine, the emf behind the reactance is generally > 1. To account for that, a correction factor can be used in (14).

Moreover, the condition $\omega_0 = 1$ pu usually holds. All simplifications above are motivated by usual assumptions and typical parameters of transmission systems. Finally, substituting frequency deviations with the expressions in (13), (12) leads to **the proposed frequency divider formula**:

$$\boxed{\boldsymbol{\omega}_B = \mathbf{1} + \mathbf{D}(\boldsymbol{\omega}_G - \mathbf{1})} \tag{14}$$

where

$$\mathbf{D} = -(\mathbf{B}_{BB} + \mathbf{B}_{B0})^{-1}\mathbf{B}_{BG} \tag{15}$$

The example and case studies discussed in the following sections show that (14) is actually accurate in the context of transient stability analysis.

C. Inclusion of Frequency Measurements

For completeness, we discuss here how the frequency divider formula (14) can be modified to include frequency measurements as provided, for example, by PMU devices, as follows. Let us assume that, apart from synchronous machine rotor speeds, also the bus voltage phasors $\bar{\boldsymbol{v}}_M$ and hence bus frequencies $\boldsymbol{\omega}_M$ are known at a given set of network buses. Such frequencies can be used to compute the remaining unknown bus frequencies. Say that $\boldsymbol{\omega}_B = [\boldsymbol{\omega}_M, \boldsymbol{\omega}_U]$, where $\boldsymbol{\omega}_U$ are the remaining unknown bus frequencies. Then, using same notation as for (1), one has:

$$\begin{bmatrix}\bar{\boldsymbol{i}}_G\\ \bar{\boldsymbol{i}}_M\\ \bar{\boldsymbol{i}}_B\end{bmatrix} = \begin{bmatrix}\bar{\mathbf{Y}}_{GG} & \bar{\mathbf{Y}}_{GM} & \bar{\mathbf{Y}}_{GU}\\ \bar{\mathbf{Y}}_{MG} & \bar{\mathbf{Y}}_{MM}+\bar{\mathbf{Y}}_{M0} & \bar{\mathbf{Y}}_{MU}\\ \bar{\mathbf{Y}}_{UG} & \bar{\mathbf{Y}}_{UM} & \bar{\mathbf{Y}}_{UU}+\bar{\mathbf{Y}}_{U0}\end{bmatrix}\begin{bmatrix}\bar{\boldsymbol{e}}_G\\ \bar{\boldsymbol{v}}_M\\ \bar{\boldsymbol{v}}_B\end{bmatrix} \tag{16}$$

and, following the same derivations discussed in the previous sectione, the frequency divider formula (14) becomes:

$$\boldsymbol{\omega}_U = -(\mathbf{B}_{UU}+\mathbf{B}_{U0})^{-1}\begin{bmatrix}\mathbf{B}_{UG} & \mathbf{B}_{UM}\end{bmatrix}\begin{bmatrix}\boldsymbol{\omega}_G\\ \boldsymbol{\omega}_M\end{bmatrix} \tag{17}$$

The expression above can be used in two ways. In simulations, one can model PMU devices and use their measures to obtain a better estimation of the frequencies at remaining buses. This is particularly relevant, in our opinion, to define the impact of noise and measurement corruptions of the PMU measure, as noise can be easily included in (17). In state-estimation, using real-world frequency measures obtained from the system to estimate frequency variations at remaning system buses. Since the focus of this paper is on the definition of the frequency divider, in the following we focus exclusively on simulations and on (14). We will further discuss the applications and practical aspects of (17).

III. Example

In this section, we illustrate the frequency divider formula (14) derived in the previous section through a simple example. Such an example will serve to illustrate why we call (14) *frequency divider* and to compare the dynamic behavior of (14) with respect to conventional washout filters as well as discuss its conceptual difference with respect to the frequency of the COI.

Let us consider the simple radial system shown in Figure 1. The lossless connection, with total reactance $x_{hk} = x_{hi} + x_{ik}$,

represents the series of the internal reactances of the machines, and series reactances of the step-up transformers and the transmission line. Hence, the frequencies at buses h and k, say ω_h and ω_k, respectively, are the rotor speeds of the synchronous generators.

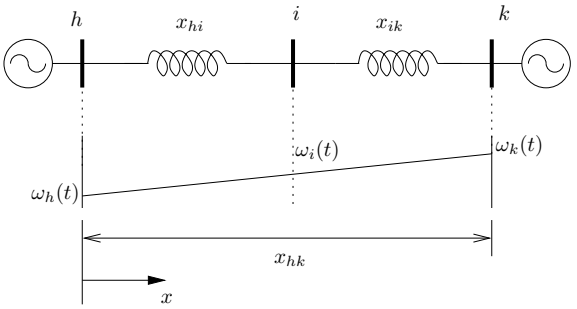

Fig. 1: Two-machine radial system.

Applying the frequency divider formula (14), we obtain:

$$\begin{aligned}\omega_i(t) &= \boldsymbol{D}\cdot\begin{bmatrix}\omega_h(t)\\ \omega_k(t)\end{bmatrix} = -(\boldsymbol{B}_{BB}+\boldsymbol{B}_{B0})^{-1}\boldsymbol{B}_{BG}\cdot\begin{bmatrix}\omega_h(t)\\ \omega_k(t)\end{bmatrix}\\ &= \left[\tfrac{1}{x_{hi}}+\tfrac{1}{x_{ik}}\right]^{-1}\begin{bmatrix}\frac{1}{x_{hi}} & \frac{1}{x_{ki}}\end{bmatrix}\cdot\begin{bmatrix}\omega_h(t)\\ \omega_k(t)\end{bmatrix} \qquad (18)\\ &= \frac{x_{ik}}{x_{hk}}\cdot\omega_h(t)+\frac{x_{hi}}{x_{hk}}\cdot\omega_k(t)\end{aligned}$$

It is worth noticing that, as a direct consequence of (14), the instantaneous frequency $\omega_i(t)$ at a generic point i between the boundaries h and k is a linear interpolation between $\omega_h(t)$ and $\omega_k(t)$ (see lower part of Fig. 1). Such a linear relation is consistent with the assumption to assume steady-state conditions in the distribution of the frequency along the transmission line. Note also that (18) has the same formal structure of the well-known voltage divider of a resistive circuit where the frequencies function as the voltage potential. Hence the name the we have chosen to define (14).

The remainder of this section discusses the accuracy of (18) through numerical simulations based on the 3-bus system shown in Fig. 2, which includes two synchronous machines and a load. The impedances of the transmission lines include the step up transformers and transmission lines ($\bar{z} = 0.025 + j0.075$ pu). We first consider a standard model for transient stability analysis where transmission lines are lumped and modeled as constant impedances and generator flux dynamics are neglected. Generators are equal and are modeled as a 6$^{\text{th}}$ order synchronous machine, a IEEE Type DC1 automatic voltage controller and a turbine governor with inclusion of servo and reheater models [27]. The load is modeled as a constant admittance. The disturbance is a three-phase fault that occurs at bus 3 at $t = 1$ s and is cleared after 150 ms by opening one of the two lines connecting buses 1 and 3.

Figure 3 shows the transient behavior of synchronous machine rotor speeds, the frequency of the COI (ω_{COI}), and the estimated frequency at the load bus using the proposed frequency divider approach. Since the inertias of the machines are equal, oscillations are averaged out from the value of ω_{COI}

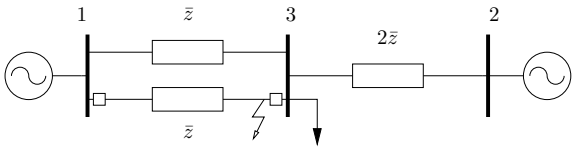

Fig. 2: 3-bus system.

as it can be readily deduced by the COI frequency expression given in Appendix I. On the other hand, the estimated bus frequency $\omega_{\text{Bus 3}}$ provided by (18) shows oscillations in phase with $\omega_{\text{Syn 1}}$, as expected, since the load bus is electrically closer to generator 1 ($x_{13} < x_{32}$). Clearly, the frequency of the COI is also unable to capture the proximity to any machine of the system. ω_{COI} can thus be used only as an indication of the overall *trend* of the system frequency but could be inadequate if utilized as a control signal for devices that regulates the frequency as those discussed in the introduction of this paper.

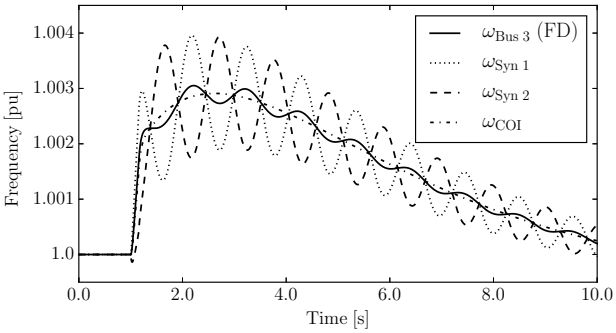

Fig. 3: 3-bus system – Synchronous machine rotor speeds, COI frequency, and frequency at bus 3 estimated based on the proposed frequency divider (FD) approach.

The model and the dynamics of the load connected to bus 3 are not included in (18) and need not to be known to define ω_3. This is one of the major differences of the proposed approach with respect to [18]. Clearly, load models and dynamics do impact on the transient behavior of the system, which includes the machines at buses 1 and 2 whose rotor speeds are required to compute ω_3. Load models are thus *implicitly* taken into account in the frequency divider formula.

We now compare the trajectories of the frequency estimation at the load bus for the 3-bus system using the proposed frequency divider and the conventional washout filter described in Appendix II. Figure 4 shows the results obtained with a more detailed model of the system considering 8$^{\text{th}}$ order models of synchronous machines and dq-frame dynamic models of the transmission lines and the load at bus 3. All parameters are the same as in Fig. 3, which is obtained using standard transient stability models. This more accurate model shows that, during the fault, the frequency drops due to the effect of machine fluxes. After the fault occurrence and clearance, the frequency also shows small high-frequency oscillations which are properly captured by (18). These oscillations cause severe numerical issues along the entire simulation in the behavior of the washout filter – see also [19] for an in-depth discussion

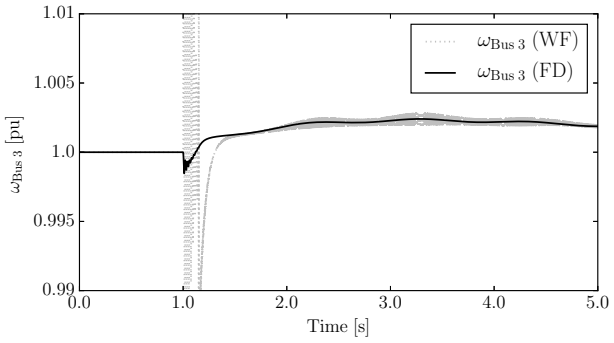

Fig. 4: 3-bus system – Frequency at bus 3 estimated with the frequency divider (FD) and the conventional washout filter (WF). The system is simulated using the fully-fledged dq-axis model.

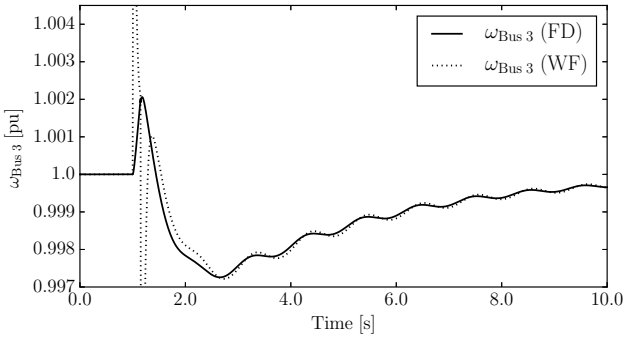

Fig. 6: 3-bus system – Frequency at bus 3 estimated with the frequency divider (FD) and the conventional washout filter (WF). The load is a squirrel cage induction motor with a 5th-order dq-axis model.

on this matter – as well as a significant delay of the filter to show the over-frequency after the line disconnection.

As indicated in Section II, one of the main assumptions on which the frequency divider formula is based, is that load currents can be neglected in (1). This is a common assumption in most analyses based on the admittance matrix, e.g., short-circuit calculations [22]. Moreover, in standard transient stability analysis, loads are approximated using constant impedances (see, for example, [28]), which, by the way, could be easily included in (14).

In the remainder of this section, we show that the effect of loads, including non-linear and dynamic ones is actually negligible for the calculation of the bus frequencies. With this aim, we consider again the dynamic response of the 3-bus system of Fig. 1 following a short-circuit at bus 3, and we substitute the constant admittance load with a static voltage- and frequency-dependent load (see Fig. 5) and a 5th-order dq-axis model of an asynchronous motor (see Fig. 6).

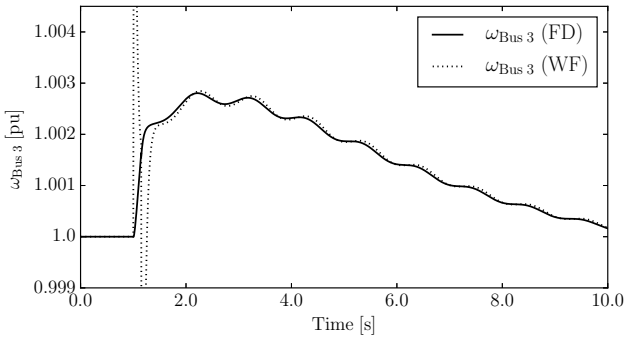

Fig. 5: 3-bus system – Frequency at bus 3 estimated with the frequency divider (FD) and the conventional washout filter (WF). The load is modeled as a frequency-dependent load representing an aluminum plant ($\alpha_p = 1.8$, $\alpha_q = 2.2$, $\beta_p = -0.3$, $\beta_q = 0.6$).

The exponential voltage- and frequency-dependent load is modeled as follows [27], [29]:

$$p_i = p_0 \left(\frac{v_i}{v_0}\right)^{\alpha_p} \omega_i^{\beta_p} \qquad (19)$$
$$q_i = q_0 \left(\frac{v_i}{v_0}\right)^{\alpha_q} \omega_i^{\beta_q}$$

In the simulations carried out to obtain Fig. 5, the frequency ω_i is estimated using the washout filter or the proposed frequency divider formula, depending on the model considered. The parameters p_0, q_0 and v_0 are the initial load active and reactive powers and voltage magnitude at bus i, respectively, determined with the power flow analysis. The parameters α_p, β_p, α_q and β_q resemble those of an aluminum plant and are based on [30]. Finally, the dynamic model of the asynchronous motor is based on [31].

Simulation results confirm that the frequency divider formula (14) is accurate as it is able to estimate the frequency at the load bus similarly to the washout filter but avoiding the numerical issues of the latter. It is interesting to note that the time evaluation of the frequency in the case of the asynchronous motor is consistently different from the static load model. The load model, in fact, does impact on the overall dynamic behavior of the system and, hence, also on the variations of rotor speeds of synchronous machines. Since the frequency divider is based on such variations, load models are indirectly taken into account in (14).

Apart from the simulations included in this section, we have considered other nonlinear load models and several different scenarios. In every test we have carried out, results, which are not shown here for space limitations, were always consistent and similar to those shown in this section. We thus conclude that the proposed frequency divider is accurate and that the approximations discussed in Section II, including that related on load models, are reasonable.

IV. Case Studies

In this section, two real-world systems are considered, namely, a 1,479-bus model of the all-island Irish transmission system; and a 21,177-bus model of the ENTSO-E transmission system. These systems are utilized to compare the performance

and accuracy of the proposed frequency divider against the results obtained using the conventional washout filter. The topology and the steady-state data of both systems are based on the actual real-world systems provided by and the Irish TSO, EirGrid, and ENTSO-E,[4] respectively. However, all dynamic data are guessed based on the knowledge of the technology of power plants.

The dynamic model of the Irish system includes both conventional and wind power generation. This system allows understanding the accuracy of the frequency divider considering a large penetration of induction machines and power electronic devices that are included in the models of wind turbines. The considered dynamic model of the ENTSO-E system includes only conventional power plants. Its large size allows comparing the computational burden of the conventional washout filter with the proposed frequency divider, i.e., number of state and algebraic variables, size and sparsity of matrices and computing times.

All simulations are obtained using Dome, a Python-based power system software tool [32]. The Dome version utilized in this case study is based on Python 3.4.1; ATLAS 3.10.1 for dense vector and matrix operations; CVXOPT 1.1.8 for sparse matrix operations; and KLU 1.3.2 for sparse matrix factorization. All simulations were executed on a 64-bit Linux Ubuntu 14.04 operating system running on a 8 core 3.60 GHz Intel Xeon with 12 GB of RAM.

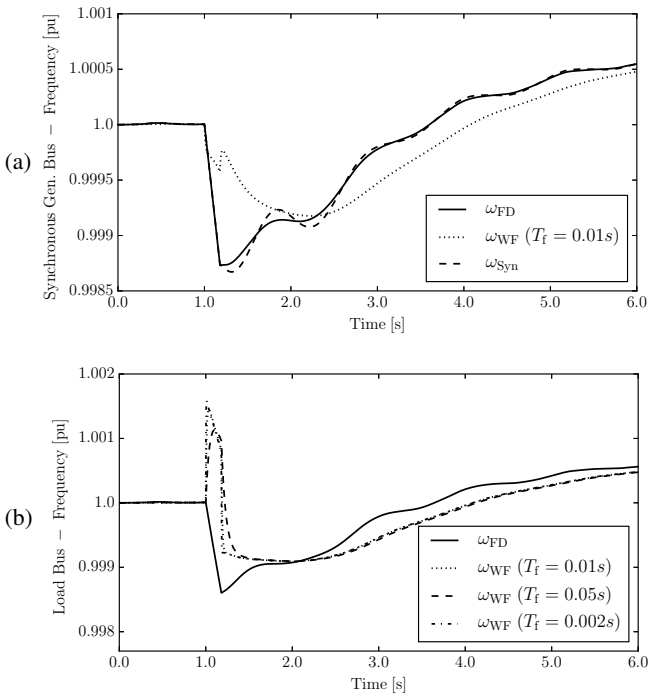

Fig. 7: Frequency response of the Irish transmission system facing a three-phase fault close to a synchronous machine: (a) Synchronous machine bus; (b) Load bus.

A. Irish Transmission System

This subsection considers a dynamic model of the all-island Irish transmission system. This includes 1,479 buses, 1,851 transmission lines and transformers, 245 loads, 22 conventional synchronous power plants modeled with 6$^{\rm th}$ order synchronous machine models with AVRs and turbine governors, 6 PSSs and 176 wind power plants, of which 34 are equipped with constant-speed (CSWT) and 142 with doubly-fed induction generators (DFIG). The large number of non-conventional generators based on induction machines and power electronics converters makes this system an excellent test-bed to check the accuracy of the proposed frequency divider.

Two scenarios are considered: Subsection IV-A.1 shows the response of the Irish system facing a three-phase fault close to both a synchronous machine and a load, whereas Subsection IV-A.2 simulates a fault close to a wind power plant.

1) Fault close to a synchronous machine and a load: A three-phase fault occurs at $t = 1$ s, and is cleared by means of the disconnection of one transmission line after 180 ms. The location of the fault is close to a synchronous machine ($S_n = 181.7$ MVA), and a load (9.72 MW and 1.16 MVAr), and their frequency is shown in Fig. 7.

Figure 7(a) depicts the rotor speed of the synchronous machine (Syn), as well as the estimated frequency of the bus where the machine is connected using both the proposed frequency divider (FD) and the washout filter (WF). The time constant of the filter is $T_f = 0.01 \simeq 3/\Omega_n$ s, which is the default value in [17]. It can be seen how the frequency divider tracks with high level of accuracy the rotor speed of the machine during and after the transient. On the other hand, the washout filter has a significant difference with respect to the rotor speed during the transient, and becomes accurate 4 s after the fault occurrence.

The frequency of a load bus close to the fault is estimated using both the frequency divider and the washout filter, and the comparison is shown in Fig. 7(b). To study how this frequency estimation is affected by the value of the filter time constant, three values are compared: the base value of $T_f = 0.01 \simeq 3/\Omega_n$ s used in the previous examples and simulations, as well as five times bigger and smaller time constants, i.e., $T_f = 0.05$ and $T_f = 0.002$ s, respectively. It can be observed that both estimators show a similar behavior about 2 s after the fault occurrence. However, the trajectories during the transient are significantly different. While the frequency divider shows a behavior similar to that of the synchronous machine rotor speed shown in Fig. 7(a), the washout filter shows a peak before the disconnection of the line that does not correspond to any physical behavior in the system.

2) Fault close to a wind power plant: In this subsection, a three-phase fault occurs close to a wind power plant, and is cleared after 240 ms (see Fig. 8). The wind plant is composed of 17 CSWTs (bus A), and 20 DFIGs split into 2 groups (buses B and C).

The frequency of bus A is estimated using both the proposed frequency divider and the filter, and the trajectories are shown in Fig. 9. The time constant of the filter is the default value of $T_f = 0.01$ s. As in the previous case, FD and WF

[4]The data of the ENTSO-E system have been licensed to the first author by ENTSO-E. Data can be requested through an on-line application at www.entsoe.eu.

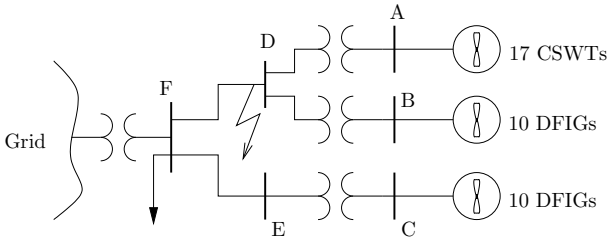

Fig. 8: Scheme of a section of the Irish transmission system that includes a wind power plant.

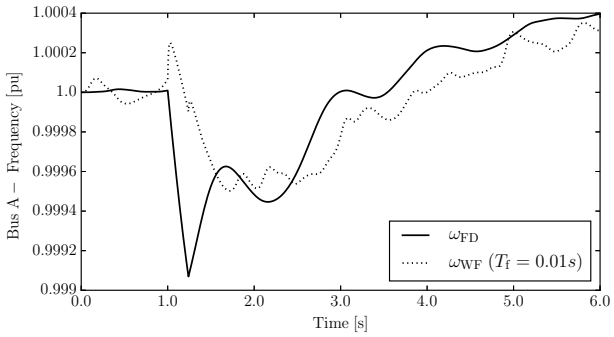

Fig. 9: Frequency response of the Irish transmission system facing a three-phase fault close to a wind power plant.

trajectories are considerably different. While the frequency divider shows a frequency response similar to the one obtained in Subsection IV-A.1, the filter adds a relatively high level of noise to the frequency measure. This is due to the fact that the washout filter estimates frequency variations based on a numerical derivative of the phase angle of the voltage at the point of connection of the wind turbine. Bus voltage angle varies in order to account for the small variations of the active power injected at the bus by the wind power plant. Such variations are a consequence of the stochastic behavior of the wind speed. However, the wind turbine does not impose the frequency at its node and, thus, the bus frequency is not related to wind turbine active power variations, as it happens for synchronous generators. Of course, the variations of the active power generation of the wind turbine do affect the dynamic behavior of synchronous machines which need to compensate the power unbalance. This is implicitly captured by the proposed frequency divider formula.

B. ENTSO-E Transmission System

This subsection considers a dynamic model of the ENTSO-E transmission system. The model includes 21,177 buses (1,212 off-line); 30,968 transmission lines and transformers (2,352 off-line); 1,144 coupling devices, i.e., zero-impedance connections (420 off-line); 15,756 loads (364 off-line); and 4,828 power plants. Of these power plants, 1,160 power plants are off-line. The system also includes 364 PSSs.

This subsection provides a comparison of the computational burden of the frequency divider and washout filters, when these are connected to all buses. The case without any frequency estimator is also considered. Results are shown in Table I.

The number of state and algebraic variables, and the size and sparsity of the state matrix in the three cases is first compared. Both the frequency divider and the washout filters add to the system a number of algebraic variables equal to the number of buses of the system. Then, each filter define two state variables per bus, whereas the proposed frequency divider does not include differential equations. This leads to an increase in the number of elements of the state matrix of 31.07 % and 105.82 % for the frequency divider and the filter, respectively. The percentage of the non-zero elements with respect to the total number of elements, is reduced by 13.28 % by using the frequency divider, while the filter decreases this number by 40.23 %.

A power flow analysis followed by the initialization of dynamic devices is then carried out. The computational time of the initialization is also reported in Table I. This consists mainly in the set-up of synchronous machines and primary regulators state and algebraic variables, and the computation of the matrix $\mathbf{D}$ or of the initial values of the variables of the washout filters, depending on the frequency estimator that is included in the model. It can be observed that both the frequency divider and the filters increase this value by 15.76% and 14.18 %, respectively.

Finally, a time domain simulation (TDS) is performed for each scenario. The simulation lasts 5 s, and the contingency considered is a three-phase fault, cleared after 200 ms. The time step of the TDS is 0.02 s. The implicit trapezoidal method is used for the time integration, and each integration step is solved by using the dishonest Newton-Raphson method [27]. Observing Table I, it can be observed that installing washout filters at every bus increases the computational time of the TDS by 18.65 %, while this time is only 10.21 % higher in the case of the proposed frequency divider.

A final important remark is the following. From the computational point of view, (14) might not be the most adequate expression to implement in practice. In fact, while $\mathbf{B}_{BB}$, $\mathbf{B}_{G0}$ and $\mathbf{B}_{BG}$ tend to be extremely sparse matrices, $\mathbf{D}$ is not. For example, Table II shows the size and number of non-zero elements of the aforementioned matrices for the ENTSO-E system. Matrix $\mathbf{D}$ is almost dense and thus its computational burden is unacceptable for large systems. Note also that the computation of $\mathbf{D}$ alone requires about 3 s.

TABLE II: Size and number of non-zeros (NNZ) elements of matrices $\mathbf{B}_{BB}$, $\mathbf{B}_{G0}$, $\mathbf{B}_{BG}$ and $\mathbf{D}$ for the ENTSO-E system.

Matrix	Size	NNZ	NNZ %
$\mathbf{B}_{BB}$	$21,177 \times 21,177$	$72,313$	0.0161
$\mathbf{B}_{BG}$	$21,177 \times 4,832$	$4,832$	0.0047
$\mathbf{B}_{G0}$	$21,177 \times 21,177$	$3,245$	0.0007
$\mathbf{B}_{BB} + \mathbf{B}_{G0}$	$21,177 \times 21,177$	$72,313$	0.0161
$\mathbf{D}$	$21,177 \times 4,832$	$86,169,456$	84.2096

For the reason above, the use of (14) is impractical for a computer-based implementation of the frequency divider and may cause memory errors on common workstations. Hence, in Dome, we have implemented an *acausal* expression, as follows:

$$\mathbf{0} = (\mathbf{B}_{BB} + \mathbf{B}_{G0}) \cdot (\boldsymbol{\omega}_B - \mathbf{1}) + \mathbf{B}_{BG} \cdot (\boldsymbol{\omega}_G - \mathbf{1}) \quad (20)$$

Equation (20), not (14), has been used to obtain the results

TABLE I: Computational burden of different bus frequency estimators.

	Base Case	Frequency Divider		Washout Filter	
Number of state variables	49,396	49,396	(0.00%)	91,750	(+85.74%)
Number of algebraic variables	96,768	117,945	(+21.88%)	117,945	(+21.88%)
Size of DAE system	146,164	167,341	(+31.07%)	209,695	(+105.82%)
NNZ % of Jacobian Matrix	0.00256	0.00222	(−13.28%)	0.00153	(−40.23%)
Initialization of full DAE [s]	0.35087	0.40617	(+15.76%)	0.40063	(+14.18%)
Time Domain Analysis [s]	37.4006	41.2198	(+10.21%)	44.3770	(+18.65%)

reported in the third column of Table I. The interested reader can find in [33] an extensive discussion on causality and its implications on the modeling of physical systems.

V. Conclusions

This paper proposes a general expression to estimate frequency variations during the transient of electric power systems. The proposed expression is derived based on standard assumptions of power system models for transient stability analysis and can be readily implemented in power system software tools for transient stability analysis. The formula is aimed at improving the accuracy of bus frequency estimation in traditional electromechanical power system models. Simulation results show that the proposed formula is accurate, numerically robust and computationally efficient.

We see several possible ways to both improve the formulation and utilize in practical applications the proposed frequency divider. The inclusion of the effect on frequency variations of electromagnetic effects as well as the transient behavior of electromechanical wave propagation appears an interesting and challenging task for future work. The coupling of the frequency divider with digital measures provided by PMU devices appears as another interesting topic. We are also keen to observe the impact of utilizing the proposed frequency estimation as input signal for frequency controllers of non-synchronous devices, such as distributed generation and flexible loads. The authors are currently working on all directions above.

Appendix I
Center of Inertia

The *center of inertia* (COI) is a weighted arithmetic average of the rotor speeds of synchronous machines that are connected to a transmission system:

$$\omega_{\text{COI}} = \frac{\sum_{j\in\mathcal{G}} H_j \omega_j}{\sum_{j\in\mathcal{G}} H_j} \tag{21}$$

where ω_j and H_j are the rotor speed and the inertia constant, respectively, of the synchronous machine j and $\mathcal{G}$ is the set of synchronous machines belonging to a given cluster.

Appendix II
Derivative of the Bus Voltage Phase Angle

The estimation of the bus frequency deviation described in this appendix is based on the numerical derivative of the angle of bus voltage phasors [34]. The frequency estimation is obtained by means of a washout and a low-pass filter, as depicted in Fig. 10. The washout filter approximates the derivative of the input signal. Differential equations are as follows:

$$\begin{aligned} \mathrm{p}x_\theta &= \frac{1}{T_f}\left(\frac{1}{\Omega_n}(\theta-\theta_0) - x_\theta\right) \\ \mathrm{p}\omega &= \frac{1}{T_\omega}(\omega_0 + \Delta\omega - \omega) \end{aligned} \tag{22}$$

where θ_0 is the initial bus voltage phase angle (e.g., the phase angle as obtained with the power flow analysis); Ω_n is the system nominal frequency in rad/s; ω_s is the synchronous frequency in pu (typically, $\omega_s = 1$ pu); T_f and T_ω are the time constants of the washout and of the low-pass filters, respectively; x_θ is the state variable of the washout filter; and $\Delta\omega = \mathrm{p}x_\theta$. $T_f = 3/\Omega_n$ s and $T_\omega = 0.05$ s are used as default values for all simulations.

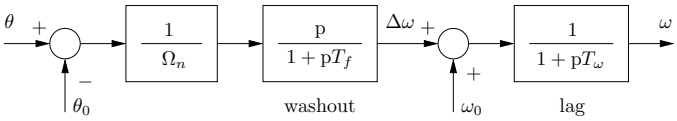

Fig. 10: Washout filter to estimate the frequency through a numerical derivative of bus voltage phase angle.

In case of polar coordinates, to compute the frequency variation $\Delta\omega$, the bus voltage phase angle θ has to be defined first. Instead of computing directly θ, which might lead to numerical issues, one can define two fictitious state variables, namely $\sin\theta$ and $\cos\theta$, whose dynamics are defined as follows [17]:

$$\begin{aligned} \mathrm{p}(\cos\theta) &= \frac{1}{T_f}(v_\mathrm{d}/v - \cos\theta) \\ \mathrm{p}(\sin\theta) &= \frac{1}{T_f}(v_\mathrm{q}/v - \sin\theta) \end{aligned} \tag{23}$$

where $v = \sqrt{v_\mathrm{d}^2 + v_\mathrm{q}^2}$. Then, $\Delta\omega$ is obtained as:

$$\Delta\omega = \begin{cases} \frac{\mathrm{p}(\sin\theta)}{\Omega_n \cos\theta}\,, & \text{if } |\cos\theta| > |\sin\theta|\,, \\ -\frac{\mathrm{p}(\cos\theta)}{\Omega_n \sin\theta}\,, & \text{otherwise.} \end{cases} \tag{24}$$

Acknowledgements

This work was conducted in the Electricity Research Center, University College Dublin, Ireland, which is supported by the Electricity Research Centers Industry Affiliates Programme (http://erc.ucd.ie/industry/). This material is based upon works supported by the Science Foundation Ireland, by funding Federico Milano and Álvaro Ortega, under Grant No.

SFI/09/SRC/E1780. The opinions, findings and conclusions or recommendations expressed in this material are those of the authors and do not necessarily reflect the views of the Science Foundation Ireland. Federico Milano is also funded by EC Marie Skłodowska-Curie Career Integration Grant No. PCIG14-GA-2013-630811.

REFERENCES

[1] O. Anaya-Lara, F. Hughes, N. Jenkins, and G. Strbac, "Contribution of DFIG-based Wind Farms to Power System Short-term Frequency Regulation," *IEE Proceedings on Generation, Transmission and Distribution*, vol. 153, no. 2, pp. 164–170, March 2006.

[2] G. Ramtharan, J. Ekanayake, and N. Jenkins, "Frequency Support from Doubly Fed Induction Generator Wind Turbines," *IET Renewable Power Generation*, vol. 1, no. 1, pp. 3–9, March 2007.

[3] J. M. Mauricio, A. Marano, A. Gómez-Expósito, and J. L. M. Ramos, "Frequency Regulation Contribution Through Variable-Speed Wind Energy Conversion Systems," *IEEE Transactions on Power Systems*, vol. 24, no. 1, pp. 173–180, Feb 2009.

[4] H. Bevrani, A. Ghosh, and G. Ledwich, "Renewable Energy Sources and Frequency Regulation: Survey and New Perspectives," *IET Renewable Power Generation, IET*, vol. 4, no. 5, pp. 438–457, September 2010.

[5] P. Moutis, A. Vassilakis, A. Sampani, and N. Hatziargyriou, "DC Switch Driven Active Power Output Control of Photovoltaic Inverters for the Provision of Frequency Regulation," *IEEE Transactions on Sustainable Energy*, vol. 6, no. 4, pp. 1485–1493, Oct 2015.

[6] K. Samarakoon, J. Ekanayake, and N. Jenkins, "Investigation of Domestic Load Control to Provide Primary Frequency Response Using Smart Meters," *IEEE Transactions on Smart Grid*, vol. 3, no. 1, pp. 282–292, March 2012.

[7] J. L. Mathieu, S. Koch, and D. S. Callaway, "State Estimation and Control of Electric Loads to Manage Real-Time Energy Imbalance," *IEEE Transactions on Power Systems*, vol. 28, no. 1, pp. 430–440, 2013.

[8] C. Taylor and S. Lefebvre, "HVDC Controls for System Dynamic Performance," *IEEE Transactions on Power Systems*, vol. 6, no. 2, pp. 743–752, May 1991.

[9] Minyuan Guan, Wulue Pan, Jing Zhang, Quanrui Hao, Jingzhou Cheng, and Xiang Zheng, "Synchronous Generator Emulation Control Strategy for Voltage Source Converter (VSC) Stations," *IEEE Transactions on Power Systems*, vol. 30, no. 6, pp. 3093–3101, Nov 2015.

[10] L. Castro and E. Acha, "On the Provision of Frequency Regulation in Low Inertia AC Grids Using HVDC Systems," *IEEE Transactions on Smart Grid*, vol. PP, no. 99, pp. 1–11, 2015.

[11] K. Yang and A. Walid, "Outage-Storage Tradeoff in Frequency Regulation for Smart Grid With Renewables," *IEEE Transactions on Smart Grid*, vol. 4, no. 1, pp. 245–252, March 2013.

[12] M. Swierczynski, D. Stroe, A.-I. Stan, R. Teodorescu, and D. Sauer, "Selection and Performance-Degradation Modeling of $LiMO_2$/Li_4 Ti_5 O_{12} and $LiFePO_4$/C Battery Cells as Suitable Energy Storage Systems for Grid Integration With Wind Power Plants: An Example for the Primary Frequency Regulation Service," *IEEE Transactions on Sustainable Energy*, vol. 5, no. 1, pp. 90–101, Jan 2014.

[13] Lu Miao, Jinyu Wen, Hailian Xie, Chengyan Yue, and Wei-Jen Lee, "Coordinated Control Strategy of Wind Turbine Generator and Energy Storage Equipment for Frequency Support," *IEEE Transactions on Industry Applications*, vol. 51, no. 4, pp. 2732–2742, July 2015.

[14] J. Winkelman, J. Chow, B. Bowler, B. Avramovic, and P. Kokotovic, "An Analysis of Interarea Dynamics of Multi-Machine Systems," *IEEE Transactions on Power Apparatus and Systems*, vol. PAS-100, no. 2, pp. 754–763, Feb 1981.

[15] M. Pavella, D. Ernst, and D. Ruiz-Vega, *Transient Stability of Power Systems – A Unified approach to Assessment and Control*. Boston: Kluwer Academic Publishers, 2000.

[16] IEEE Task Force on Load Representation for Dynamic Performance, "Load Representation for Dynamic Performance Analysis [of Power Systems]," *IEEE Transactions on Power Systems*, vol. 8, no. 2, pp. 472–482, May 1993.

[17] DIgSILENT, *PowerFactory Technical Reference Ver. 15*, Gomaringen, Germany, 2015.

[18] J. Nutaro and V. Protopopescu, "Calculating Frequency at Loads in Simulations of Electro-Mechanical Transients," *IEEE Transactions on Smart Grid*, vol. 3, no. 1, pp. 233–240, March 2012.

[19] C.-S. Hsu, M.-S. Chen, and W. Lee, "Approach for Bus Frequency Estimating in Power System Simulations," *IEE Proceedings-Generation, Transmission and Distribution*, vol. 145, no. 4, pp. 431–435, Jul 1998.

[20] A. Semlyen, "Analysis of Disturbance Propagation in Power Systems Based on a Homogeneous Dynamic Model," *IEEE Transactions on Power Apparatus and Systems*, vol. PAS-93, no. 2, pp. 676–684, March 1974.

[21] ——, "Effect of Nonuniformity on the Continuous Representation of Electromechanical Dynamics in Large Power Systems," *IEEE Power Engineering Review*, vol. 18, no. 5, pp. 60–61, May 1998.

[22] P. M. Anderson, *Analysis of Faulted Power Systems*. New York, NY: Wiley-IEEE Press, 1995.

[23] "ABB Simpow," STRI, available at http://www.stri.se.

[24] A. Yazdani and R. Iravani, *Voltage-Sourced Converters in Power Systems*. New York: IEEE Press – John Wiley & Sons, 2010.

[25] T. Demiray, G. Andersson, and L. Busarello, "Evaluation Study for the Simulation of Power System Transients using Dynamic Phasor Models," in *2008 IEEE/PES Transmission and Distribution Conference and Exposition: Latin America*, Aug 2008, pp. 1–6.

[26] S. Almer and U. Jonsson, "Dynamic Phasor Analysis of Periodic Systems," *IEEE Transactions on Automatic Control*, vol. 54, no. 8, pp. 2007–2012, Aug 2009.

[27] F. Milano, *Power System Modelling and Scripting*. London: Springer, 2010.

[28] P. M. Anderson and A. A. Fouad, *Power System Control and Stability*. New York, NY: Wiley-IEEE Press, 2002.

[29] P. Hirsch, *Extended Transient-Midterm Stability Program (ETMSP) Ver. 3.1: User's Manual*, EPRI, TR-102004-V2R1, May 1994.

[30] G. L. Berg, "Power System Load Representation," *Proceedings of the IEEE*, vol. 120, no. 3, pp. 344–348, 1973.

[31] P. C. Krause, O. Wasynczuk, and S. D. Sudhoff, *Analysis of Electric Machinery and Drive Systems*. New York: John Wiley & Sons, 2002, 2nd Edition.

[32] F. Milano, "A Python-based Software Tool for Power System Analysis," in *Procs. of the IEEE PES General Meeting*, Vancouver, BC, Jul. 2013.

[33] M. M. Tiller, *Introduction to Physical Modeling with Modelica*. Boston: Kluwer Academic Publishers, 2001.

[34] IEEE Task Force on Load Representation for Dynamic Performance, "Load Representation for Dynamic Performance Analysis [of Power Systems]," *IEEE Transactions on Power Systems*, vol. 8, no. 2, pp. 472–482, May 1993.

Federico Milano (S'02, M'04, SM'09, F'16) received from the Univ. of Genoa, Italy, the ME and Ph.D. in Electrical Eng. in 1999 and 2003, respectively. From 2001 to 2002 he was with the Univ. of Waterloo, Canada, as a Visiting Scholar. From 2003 to 2013, he was with the Univ. of Castilla-La Mancha, Spain. In 2013, he joined the Univ. College Dublin, Ireland, where he is currently Professor of Power System Control and Protections. His research interests include power system modeling, stability analysis and control.

Álvaro Ortega (S'14) received from Escuela Superior de Ingenieros Industriales, University of Castilla-La Mancha, Ciudad Real, Spain, the degree in Industrial Engineering in 2013, with a final project on modeling and dynamic analysis of compressed air energy storage systems. Since September 2013, he is a Ph.D. student candidate with the Electricity Research Center, University College Dublin, Ireland.

This Article is part of a project that has received funding from the **European Union's Horizon 2020 research and innovation programme under grant agreement Nº727481**